Lasers in Manufacturing Conference 2015

Keyhole shape and element loss in laser beam welding of brass alloys

Florian Hugger[a]*, Vincent Mann[a], Matthias Holzer[a], Stephan Roth[a,c], Michael Schmidt[a,b,c]

[a]*Bayerisches Laserzentrum GmbH, Konrad-Zuse-Str. 2-6, Erlangen 91052, Germany*
[b]*Institute of Photonic Technologies, Friedrich-Alexander-Universität Erlangen-Nürnberg, Konrad-Zuse-Str. 3-5, Erlangen 91052, Germany*
[c]*Erlanger Graduate School in Advanced Optical Technologies, Paul-Gordan-Str. 6, Erlangen 91052, Germany*

Abstract

Deep penetration laser beam welding is characterized by a keyhole where evaporation of the material takes place. Welding alloys with a significant difference of evaporation temperature of base material and alloying elements leads to disproportionately high evaporation of the volatile element. This leads to elongation of the keyhole and loss of the volatile element in the weld.
In this paper full penetration welds of brass alloys of 10%, 20% and 37% zinc by mass are carried out using a solid state laser. The welding process is detected by high-speed imaging by which vapor capillary elongation as well as capillary shape is observed for different parameters. Furthermore alloy composition is analyzed and element loss depending upon alloy composition and feed rate is detected by EDX measurement.

Keywords: Laser beam welding, copper alloys, evaporaton

1. Volatile element evaporation

Laser beam deep penetration welding is characterized by a vapor capillary, which is formed in the melt pool. At the surface of the vapor capillary, which usually has dimensions of the laser beam diameter, the material evaporates. Nevertheless due to different evaporation temperatures of different alloying elements the evaporation is not homogeneous as volatile elements develop high evaporation pressures, which increase evaporation rate and therefore loss of volatile elements in the weld. These phenomena regarding evaporation process of different alloying systems and element loss have been investigated in the past and theories have been developed to calculate element loss for different metal alloys.

In literature significant evaporation and loss of volatile elements in material systems Fe-Mn, Al-Mg and Al-Zn is reported. Collur et al., 1987 investigated evaporation of manganese in high manganese containing stainless steel at conduction mode welding with a CO_2-laser. Three different steps are defined. First a transport of alloying elements from the bulk material to the melt surface, followed by evaporation at the surface which is dependent upon surface temperature distribution and activity of surface elements. Finally, element loss is dependent upon a transportation mechanism from the liquid to the gaseous phase which is characterized by the boundary layer at the liquid surface. It was shown that the evaporation rate is not significantly influenced by shielding gases and the dominant step is the evaporation reaction at the surface. Evaporation rate is a function of temperature of the melt pool, though only temperatures near to the melting temperature were investigated.

Mundra and Debroy, 1993 developed a theoretical model to predict the evaporation rates of different alloying elements. The evaporation rate of an alloying element $J_{p,i}$ is proportional to its partial pressure p_i^0 over the evaporating surface (equation 1). a_i is the activity of an alloying element at the melt surface, P_l is the equilibrium vapor pressure at the melt surface, M_i is molecular weight of species i, M_v is the molecular weight of the vapor and J_p is the total evaporation rate.

$$J_{p,i} = a_i \frac{p_i^0}{P_l} \frac{M_i}{M_v} J_p \qquad (1)$$

The total evaporation rate was calculated by multiplying the density of the vapor, the Mach number and the local speed of sound in the vapor at evaporation temperature. Results of calculations and experiments for stainless steel with high manganese content correlate well for fractions of evaporating alloying elements. Nevertheless the total evaporation rate is overestimated by factor of 3.

Dilthey et al., 2001 investigated volatile element evaporation in deep penetration welding in which the evaporation process is controlled by two simultaneous processes as there is evaporation at the vapor capillary surface and diffusion of volatile elements from melt pool towards the evaporating surface. It is shown that the evaporation process is the dominant step and that depletion of volatile elements is reduced at high welding speed. Exceeding a feed rate of 10 mm/s leads to loss of magnesium and zinc of less than 10% of base material alloy composition for different aluminum alloys. Higher feed rate resulted in decreasing element loss which was also reported in Khan et al., 1988.

Jandaghi et al., 2008 investigated the evaporation of alloying elements of stainless steel 1.4401 at laser beam spot welding in dependency of laser pulse power and duration. It is shown that that there is a decrease of chromium and manganese with increasing laser pulse duration and power density.

Huber, 2014 showed that the loss of magnesium in aluminum-magnesium alloys increases to a threshold value of 4 m% Mg and decreases from this value with increasing magnesium content in the material, though the fraction of magnesium in the vapor continuously increases. Therefore it is assumed that at a certain threshold the vapor is saturated and no further evaporation of volatile element occurs.

The investigations reported in literature used alloys with volatile element fractions less than 10% by mass and the feed rate during welding was below 50 mm/s. In order to the understand the element evaporation when welding high alloyed materials at high feed rates, the reported experiments here use concentrations up to 37% by mass of volatile elements and feed rates up to 200 mm/s. Previous investigations carried out with CuZn37 showed shape changes of the vapor capillary from a spherical shape at low welding speed to an elliptical shape at high feed rates. At a feed rate of 15 m/min the vapor capillary has an aspect ratio of length to width larger than five. This phenomenon was drawn to the fact that at the sides of the capillary significant evaporation occurs which keeps the capillary open Hugger et al., 2014. Up to now vapor capillary elongation in dependency of volatile element content is not investigated.

2. Experimental setup

Laser beam welding experiments were carried out using a disk laser with wavelength of 1,030 nm and maximal output power of 3.5 kW. The laser beam was focused to a diameter of 340 µm in focal plane and deflected with a scanner. Different brass alloys with 10%, 20% and 37% zinc by mass with 1 mm sheet thickness were used. The process was observed by a high-speed camera which was tilted 60° in relation to plain of welding area to investigate capillary elongation and shape. The camera was directed in leading direction that the vapor capillary front, capillary and melt pool could be observed. The element concentration of zinc in welded zone was determined by EDX measurement. All experiments were repeated three times.

3. Results and discussion

3.1. Vapor capillary elongation

Welding CuZn37 with different laser powers and feed rates shows a significant elongation of the vapor capillary with increasing feed rate, see figure 1. The laser power has no clear and significant influence upon capillary elongation. With increasing feed rate the capillary length increases from 1.2 mm at 33 mm/s to 2.4 mm at 200 mm/s. At 33 mm/s a longer capillary is measured at a lower laser power while at 66 mm/s the vapor capillary is slightly longer at higher laser power. Feed rate clearly influences vapor capillary elongation.

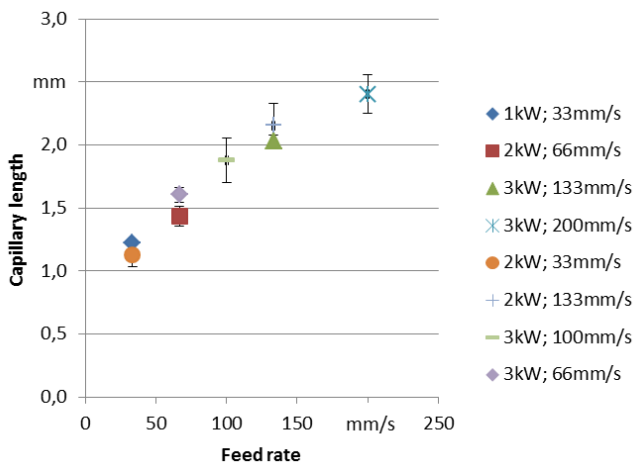

Fig. 1. Influence of feed rate and laser power upon vapor capillary length for CuZn3. N=3

For CuZn20 welding behavior is similar to CuZn37, see figure 2. It is observed that here also vapor capillary is elongated to 2.4 mm at 200 mm/s. For a laser power of 1 kW no full penetration of the material occurred.

Welding CuZn10 also resulted in an elongation of the vapor capillary, but at 66 mm/s a saturation of the capillary length is reached, see figure 3. An increased feed rate had no influence upon capillary elongation and a length of 1.6 mm is not exceeded. For 133 mm/s no stationary full penetration of the vapor capillary occurred. For welding CuZn10 a higher laser power was necessary, since absorption decreases and heat

conductivity increases with a reduced content of zinc. Both effects lead to an increase of laser power to reach full penetration of the vapor capillary.

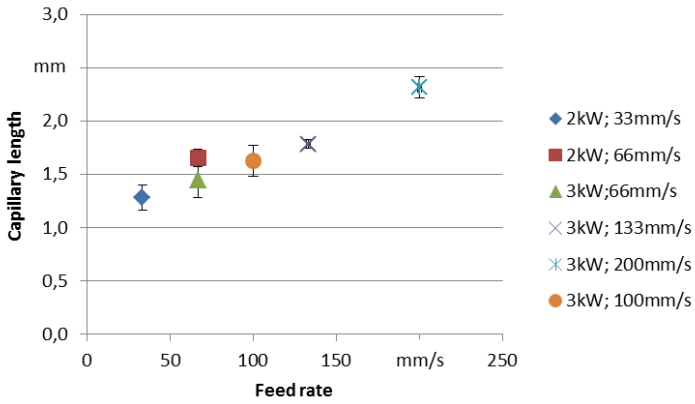

Fig. 2. Influence of feed rate and laser power upon vapor capillary length for CuZn20. N=3

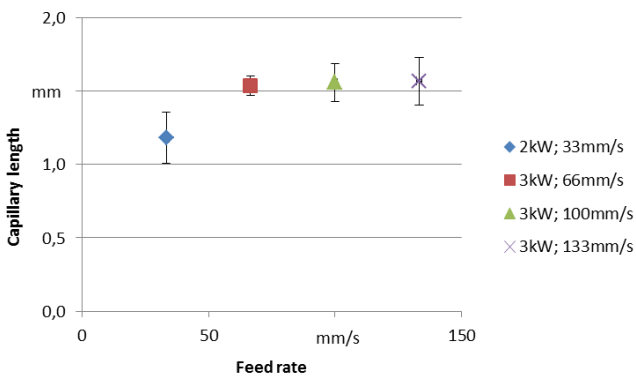

Fig. 3. Influence of feed rate and laser power upon vapor capillary length for CuZn20. N=3

Figure 4 shows the influence of the zinc content upon capillary length for different feed rates. For 66 mm/s no significant elongation with increasing zinc content is observed, while at a feed rate of 100 mm/s increased vapor capillary lengths occur for increasing zinc contents.

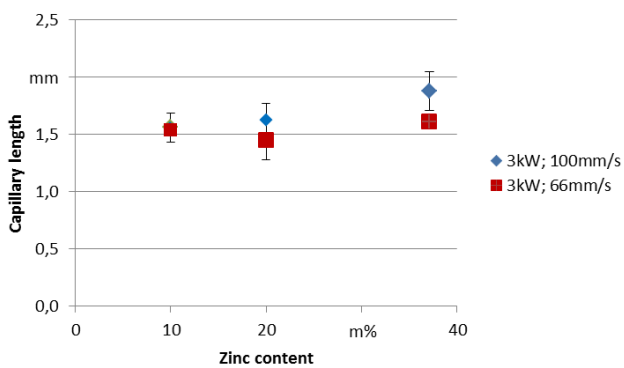

Fig. 4. Influence of zinc content upon vapor capillary length for constant laser power and different feed rates. N=3

3.2. Vapor capillary shape

Vapor capillary shape for welding CuZn37 have been observed for low feed rate of 33 mm/s and high feed rate of 100 mm/s, see figure 5. The area of the vapor capillary is colored blue, while melt pool shape is colored white. For laser power of 2 kW and feed rate of 33 mm/s the vapor capillary is slightly elongated with almost spherical shape and the melt pool has similar length compared to the capillary. For laser power of 3 kW and feed rate of 100 mm/s vapor capillary has a clear elongated drop shape. The melt pool is short compared to the capillary length. At higher feed rates the elongated drop shape of the vapor capillary becomes more pronounced.

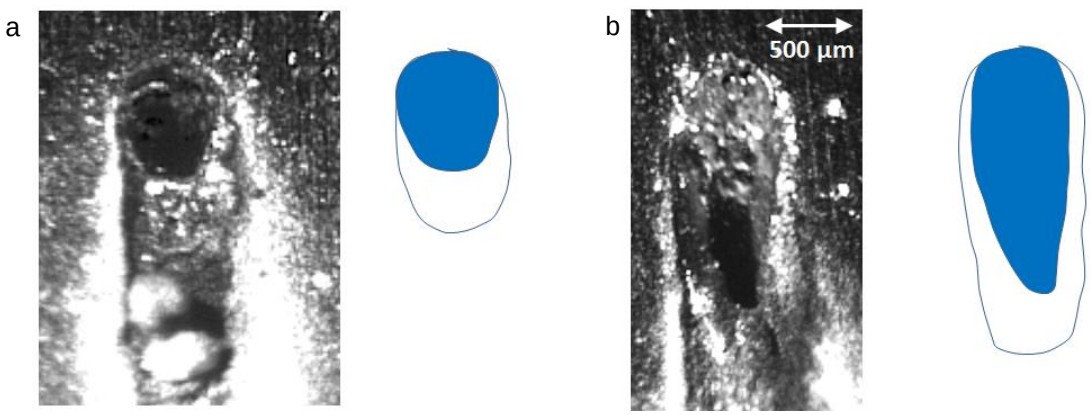

Fig. 5. Vapor capillary shape for welding CuZn37 at (a) 2 kW and 33 mm/s and (b) 3 kW and 100 mm/s

Figure 6 shows the vapor capillary shape during the welding process of CuZn20 and CuZn10 welded with parameters 3 kW and 100 mm/s. Compared to CuZn37 the capillary of CuZn20 is shorter and elliptical while the melt pool behind the capillary is longer. The weld pool of CuZn20 is wider due to higher heat conductivity in relation to CuZn37. For CuZn10 an even wider melt pool is observed while the capillary is shorter. This is attributed to a lower evaporation and higher heat conductivity of CuZn10 (184 W/(m*K)) compared to CuZn20 (142 W/(m*K)) and CuZn37 (120 W/(m*K)).

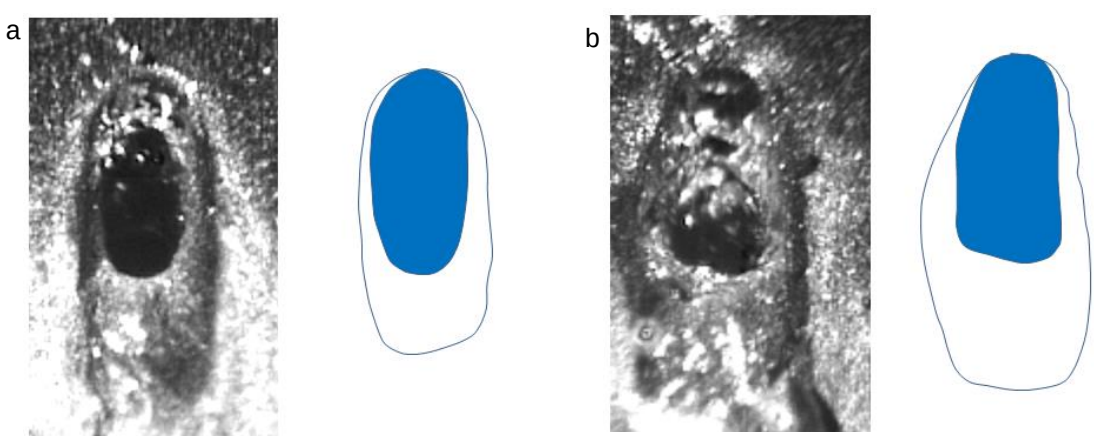

Fig. 6. Vapor capillary shape welding CuZn37 at (a) CuZn20 (b) CuZn10 at 3 kW and 100 mm/s

3.3. Element loss in weld zone

Figure 7 shows the zinc distribution in weld zone of CuZn37 welded with 2 kW and feed rate of 33 mm/s measured with an EDX-line-scan. Here an element loss of about 5 % Zn by mass in the fusion zone can be observed. Dispersion of measured points is attributed to relative error of EDX method and to micro segregation (Dilthey et al., 2001). This was the maximum element loss of zinc measured for all samples. With increasing feed rate decreasing zinc depletion occurred, see figure 8. At a high feed rate of 200 mm/s only low depletion in fusion zone is detectable.

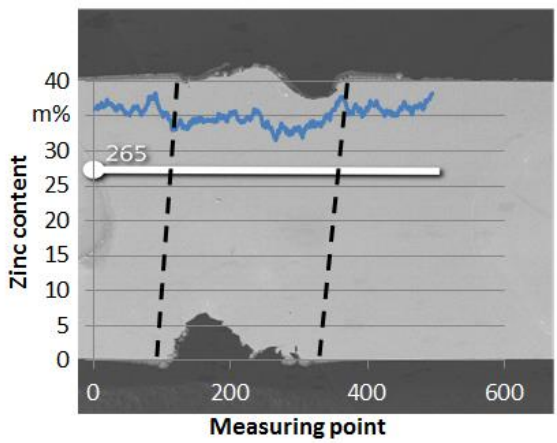

Fig. 7. Zinc content in weld zone of CuZn37 welded with2 kW and 33 mm/s

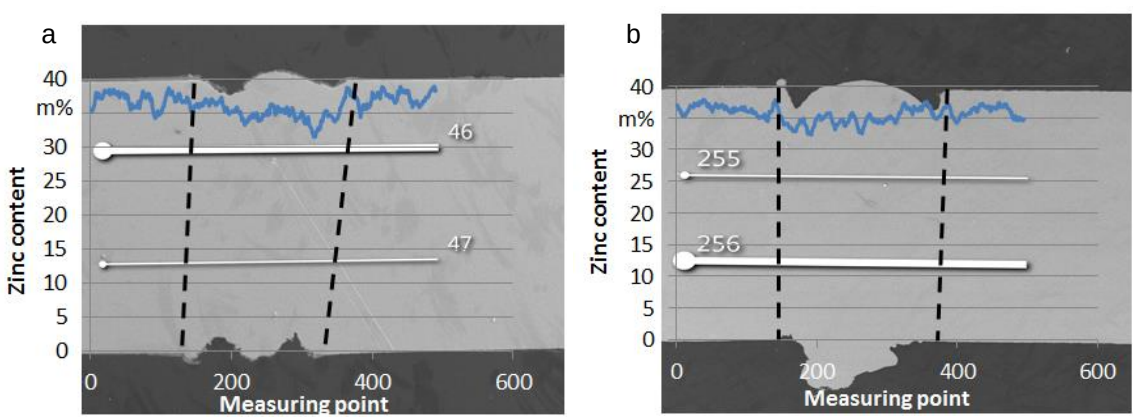

Fig. 8: Zinc content in weld zone of CuZn37 welded with (a) 3 kW and 66 mm/s and (b) 3 kW and 200 mm/s

The behavior described for CuZn37 is similar for material CuZn20 where zinc loss in fusion zone less 3% Zn by mass is observed. At feed rates higher than 66 mm/s element loss is hardly distinguishable from natural dispersions, see figure 9.

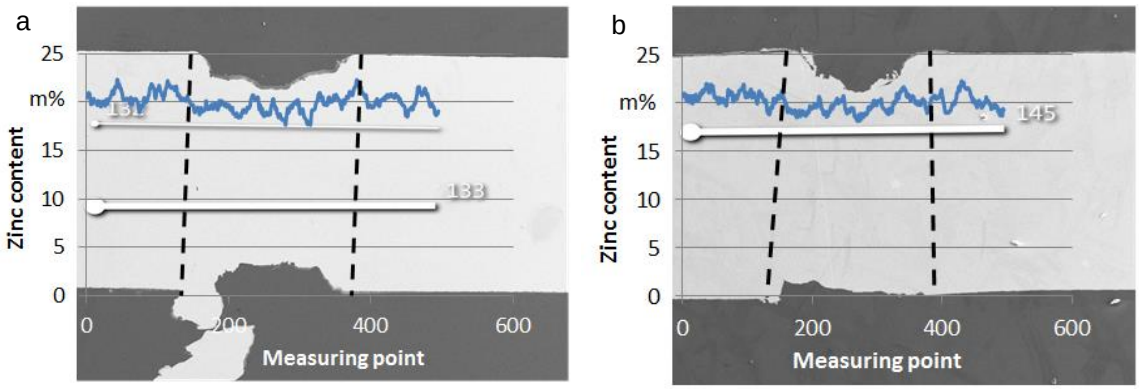

Fig. 9. Zinc content in weld zone of CuZn20 welded with (a) 2 kW and 33 mm/s and (b) 3 kW and 66 mm/s

Figure 10 shows zinc content in weld zone of CuZn10 welded with 2 kW and 33 mm/s. It is observed that zinc content in fusion zone is about 3 % Zn by mass lower compared to the base material.

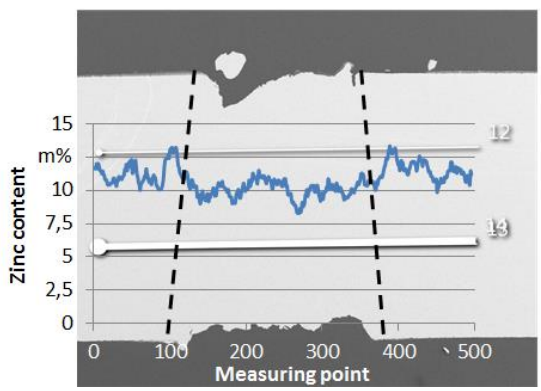

Fig. 10. Zinc content in weld zone of CuZn10 welded with 2 kW and 33 mm/s

3.4. Discussion

Experimental investigation shows that vapor capillary elongation is dependent upon content of volatile elements and feed rate. It is assumed that also at the sides of the vapor capillary significant evaporation occurs which keeps the capillary open and leads to an elongation. From comparison of vapor pressures for different brass alloys displayed in figure 11 and equation (1) it is concluded that the vapor should consist nearly completely of zinc, as the ratio of vapor pressures of zinc and copper is >>1. Since element loss is always lower than 5% Zn by mass it is supposed that total amount of evaporation rate is low and the vapor is close to saturation like reported in Huber, 2014. At saturation state all evaporated material condensates again.

Stagnating vapor capillary elongation for feed rate larger than 66 mm/s at welding CuZn10 can be explained by higher melt temperature necessary for keeping vapor pressure above ambient temperature. It is supposed that capillary closes when temperature of capillary sides fall below 1,300 °C, see figure 11. For

CuZn37 and CuZn20 vapor pressure is above ambient pressure until temperature drops below 1,100 °C for CuZn37 and 1,150 °C for CuZn20, respectively and therefore capillary is kept open for increasing distance to interaction zone with laser beam. Therefore increased capillary elongation occurs at CuZn37 and CuZn20 in comparison to CuZn10, while melt pool length is similar for all zinc alloys.

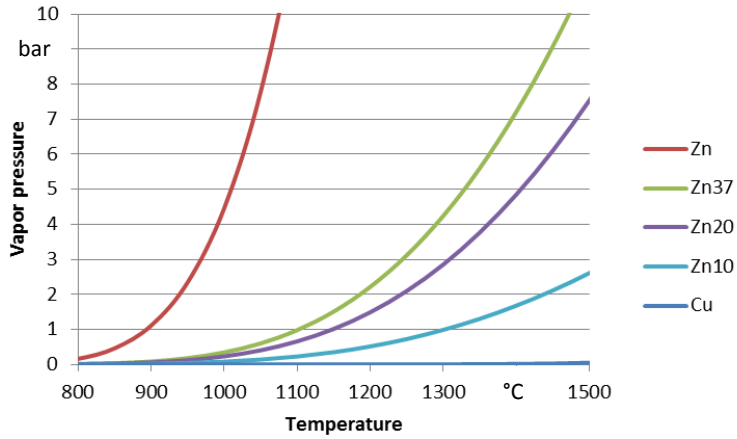

Fig. 11. Influence of temperature upon vapor pressure for different brass alloys

Figure 12 shows a sketch in which temperate distribution in weld zones of CuZn37 and CuZn10 is displayed. The capillary is colored blue and the melt pool is colored red. A linear decrease of temperature from vapor capillary front to melt pool end is assumed. For CuZn37 vapor pressure is above ambient pressure until temperature drops below 1,100 °C and therefore the capillary is kept open for a larger temperature interval. For CuZn10 the capillary closes when temperature of the capillary sides falls below 1,300 °C. It is concluded that even at higher feed rates the vapor pressure developed from CuZn10 is too low to keep the capillary open and form considerable capillary elongation. For CuZn37 the melt pool exists longer compared to CuZn10, since melting temperature is about 900 °C for CuZn37 and about 1,050 °C for CuZn10.

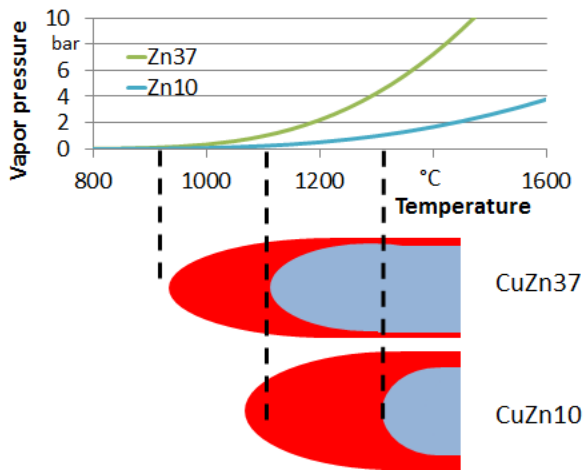

Fig. 12. Sketch of capillary elongation dependent upon temperature distribution for CuZn37 and CuZn10

4. Conclusion and outlook

For laser beam welding of brass alloys a significant elongation of the vapor capillary is observed at high feed rates. For CuZn10 the vapor capillary elongation stagnates above a feed rate of 66 mm/s. For CuZn20 and CuZn37 the capillary shows increasing elongation for whole parameter range up to 200 mm/s. The vapor capillary shape changes from spherical shape at low feed rates to elongated drop shape at high feed rates. For the same parameters the vapor capillary is drop shaped with small melt pool for CuZn37 while the capillary is more elliptic for CuZn20 and CuZn10 and the melt pool increases. For all brass materials EDX measurements show an element loss less than 5% Zn by mass. This leads to the conclusion that vapor is close to saturated state at the evaporating capillary surface since vapor should consist completely of zinc.

Further investigation will concentrate on the development of a numerical model to calculate the temperature distribution in weld zone. This model should help to understand the mechanisms of selective evaporation of volatile elements in the interaction zone of melt and laser beam and the capillary stabilization in the area behind the interaction zone where the vapor capillary is kept open without direct laser beam irradiation.

References

Collur, M.M., Paul, A, Debroy, T., 1987. Mechanism of alloying element vaporization during laser welding. Metallurgical Transactions B 18B, p. 733-740.

Dilthey, U., Gumeniouk, A., Lopota, V., Turichin, G., Valditseva, E., 2001. Development of a theory for alloying element losses during laser beam welding. Journal of Applied Physics 34, p. 81-86.

Huber, S., 2014. In-Situ-Legierungsbestimmung beim Laserstrahlschweißen. Dissertation Technische Universität München.

Hugger, F., Hofmann, K., Stein, S., Schmidt, M., 2014. Laser beam welding of brass. Physics Procedia 56, p. 576-581.

Jandaghi, M., Pavin, P., Torkamany, M.J., Sabbaghzadeh, J., 2008. Alloying element losses in pulsed Nd:YAG laser welding of stainless steel 316. Journal of Applied Physics D 41, p. 1-9.

Khan, P.A.A., Debroy, T., David, S.A., 1988. Laser beam welding of high-manganese stainless steels - examination of alloying element loss and microstructural changes. Welding Journal, p.1-7.

Mundra, K., Debroy, T., 1993. Toward understanding alloying element vaporization during laser beam welding of stainless steel. Welding Journal, p. 1-9.